77th International Astronautical Congress (IAC), Antalya, Türkiye, 29 September - 03 October 2026.
Copyright © 2026 by Mehmed Yüksel. Published by the International Astronautical Federation (IAF), with permission and released to the IAF to publish in all forms. All rights reserved.
IAC–26–A3,2C,3,x109024

LuNiS: Experimental Validation of an AI-Enabled Micro-Rover for Future Lunar Missions with Night Survival Capability

Mehmed Yüksel[1*], **Wiebke Brinkmann**[1], **Hilmi Dogu Kücüker**[1], **Zhongqian Zhao**[1], **Jakob Wehnes**[1], **Jonas Eisenmenger**[1], **Leon Spies**[2], **Joel Guetzlaff**[2], **Markus Czupalla**[2]

[1] *Robotics Innovation Center (RIC), German Reseach Center for Artificial Intelligence (DFKI) GmbH, Robert-Hooke-Str. 1, 28357, Bremen, Germany, name.surname@dfki.de*
[2] *Fachhochschule Aachen, Department for Aerospace Engineering, Hohenstaufenallee 6, 52064 Aachen, Germany,*
[*] *Contact Author:* ***Mehmed Yüksel*** *(mehmed.yueksel@dfki.de)*

Abstract

Micro-rovers represent a promising class of robotic systems for future lunar exploration missions. Such platforms can offer a cost-effective and economically scalable solution that enables reduced mission expenditure. At the same time, they maintain versatile surface-operation capabilities in constrained environments while remaining lightweight and compact. Within the joint research project SAMLER-KI, a **Lu**nar micro rover for **Ni**ght **S**urvival called LuNiS is under development and can be used for future lunar exploration tasks. The project comprises three rover variants and explores three complementary perspectives addressing the development of a complex micro-rover system: a virtual model, representing LuNiS as a space variant equipped with space-qualified components; the LuNiS Demonstration Model (DM), serving as the terrestrial testbed; and the LuNiS thermal model (TM), a thermal rover designed for environmental testing. The LuNiS-DM, developed by the German Research Center for Artificial Intelligence (DFKI), enables the validation of subsystems, software architectures, and artificial intelligence components through a variety of field and laboratory experiments. The LuNiS-TM, developed by FH Aachen University of Applied Sciences, undergoes extensive testing in a thermal vacuum chamber to evaluate the thermal design concept and to validate the underlying thermal modelling and simulations. Insights and results obtained from both rover platforms are fed directly into the design and validation process of the space variant, supporting the optimization of its thermal resilience and operational survivability during the lunar night. This paper presents the design and testing methodologies of DM and TM, and illustrates how their results contribute to the development of the final LuNiS space variant for robust lunar surface operation.

1. Introduction

Over the past decade, lunar exploration has been reshaped by the entry of private companies under the emerging "New Space" paradigm. Commercial actors such as ispace[1] and Astrobotic[2] have demonstrated that lunar-class missions can be conceived, developed, and flown outside traditional national space agency structures, typically at a fraction of the cost and development timeline of legacy programs. This shift has been enabled less by any single technological breakthrough than by a broader systems-level rethinking: the adoption of commercial-off-the-shelf (COTS) components, miniaturized and modular subsystem architectures, and design philosophies favoring lightweight, resource-efficient solutions over the large, heavy, highly bespoke systems that characterized earlier exploration eras.

The SAMLER-KI project approaches this shift from a resource-optimization perspective on lunar missions. It looks beyond the current concentration of interest on the lunar south pole toward equatorial regions as a potential focus area for a subsequent, more advanced phase of lunar surface exploration. Accordingly, the project targets the

Copyright © 2026 by Mehmed Yüksel. Published by the International Astronautical Federation (IAF), with permission and released to the IAF to publish in all forms. All rights reserved.

definition of the necessary system and subsystem architecture, together with subsystem-level technology readiness level (TRL) maturation, and the design of an AI-assisted, semi-autonomous rover system.

The functional demonstrator developed for this purpose, LuNiS (see in Fig. 1), is a pioneering system in its class in terms of size, mass, and power consumption. Equally central to this work is its targeted capability, achieved through dedicated thermal design/optimization and system-level configuration, to operate in equatorial regions and survive the lunar night without relying on radioisotope thermoelectric generators (RTG) or radioisotope heating units (RHU). Energy harvested via solar power during the lunar day is stored and used both for locomotion and to sustain the system through the lunar nights, corresponding to approximately 14 Earth days. Building on results achieved in previous phases of the project, this paper presents the new results in comparison with those earlier outcomes, demonstrating concrete progress.

2. Mission Design and Analysis

The main purpose of the mission design is to provide a structured baseline for the next phases of design and development of the rover, while keeping the flexibility and adaptability for different types of payloads and scientific objectives. For that purpose, previous planetary missions and payloads were investigated in order to derive the constraints and the variables for the design at first. Then, the research about scientifically valuable landing sites [3] for future missions was undertaken, while taking the terrain slope and roughness into account. As a result, the mission scenario was selected as taking magnetic measurements on Reiner Gamma [4] to investigate the magnetic anomalies there [5].

The following step is the generation of possible trajectories in the Reiner Gamma region to simulate the rover model with high fidelity. After the determination of region of interest, as displayed in Figure 2, the height map was derived using Digital Shape Kernel (DSK) of Reiner Gamma terrain [6] with 59 m precision in NAIF SPICE Toolkit, through which we can achieve the position of Sun and ground station locations on Earth and utilize them in time-series analysis and simulations [7] [8]. In this phase, 5000 different trajectories were generated, in order to foresee the possible outcomes of the traverse, especially in the design perspective, and to estimate the design parameters and margins. The overview of generated trajectories is also provided in Figure 2.

Then the model simulation framework was developed alongside the determination of mission phases, the rover state machine, and the submodules required for the successful mission execution. After embedding the NAIF SPICE toolkit and generated trajectories into the framework, the overall rover behavior was simulated, merging the pre-defined rover behavior procedure. As a result, we were able to achieve: (1) the amount of battery that is required for daytime operations and night-time survivability; (2) the number of solar cells required; (3) the amount of data to be downloaded; (4) the required communication bandwidth; (5) size of the mass memory unit.

3. LuNiS System

The LuNiS system can be divided into three variants. LuNiS V1 is the first iteration of the actual space model to be used for the mission (see in Fig. 1). LuNiS DM is the demonstration model and therefore the terrestrial variant of LuNiS, which was used to conduct functional tests within the project. LuNiS TM is the thermal model that underwent specialized thermal tests to validate the thermal analyses that were performed.

3.1 LuNiS V1 (space variant)

For the first iteration of the rover, LuNiS V1, the main design drivers were a specified maximum mass of 20 kg and the requirement to survive one lunar night. To achieve both goals at the same time, a design was adopted that uses secondary batteries for daytime operation and primary batteries to survive the lunar night. To ensure the thermal survival of the rover, the body was constructed from a lightweight outer body and an insulated inner body, which houses the electronics and batteries. In addition, two layers, internal and external, of Multilayer insulation (MLI) were used for insulation to further optimize thermal management. To dissipate heat from the rover during the day, thermal switches were installed to connect the inner body to a radiator on a top panel. Spring-loaded solar panels are attached to the top panel and can be deployed after mission launch to generate power for the rover. A stereo camera on the front of the rover is used for navigation, obstacle detection and avoidance, and an external payload can be attached to the rear. For mobility, a chassis with a passive swing axle is used in the rear to allow movement over un-

Copyright © 2026 by Mehmed Yüksel. Published by the International Astronautical Federation (IAF), with permission and released to the IAF to publish in all forms. All rights reserved.

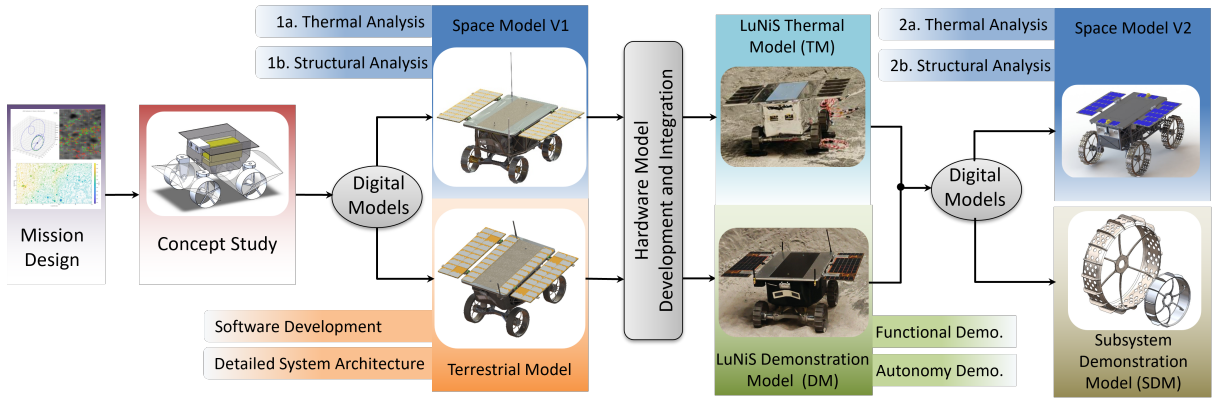


Fig. 1. SAMLER-KI project development workflow

even terrain. The entire design exists only as a theoretical CAD model, which is shown in the Fig. 1. Further details regarding this variant are provided in the preceding article [4].

3.2 LuNiS Demonstration Model (DM)

Based on the LuNiS V1 design, a demonstration model was developed, which has been manufactured and can be used for actual functional tests. Since this is a terrestrial variant, no space-grade parts were used, but only the concept, dimensions and mass of the space variant were taken into account. The mechanical structure of the DM can be divided into four main assemblies: the chassis (Fig. 3 - *left*), the external frame (Fig. 3 - *middle left*), the inner frame (Fig. 3 - *middle right*), and the top frame (Fig. 3 - *right*).

The chassis constitutes the locomotion platform of the rover. Its load-bearing structure was designed based on finite-element analysis (FEA) and topology optimization and subsequently manufactured using selective laser melting (SLM) from AlSi10Mg aluminum alloy. This approach enables a lightweight structure with sufficient stiffness and strength while allowing geometrically complex load paths to be realized. The wheels were manufactured using SLM from Ti-6Al-4V (Titanium Grade 5). Their modular interface allows individual wheels to be exchanged and different wheel configurations to be evaluated during terrestrial trials. Each drive unit combines a brushless DC (BLDC) motor with a planetary gearbox. In addition, a passive joint is incorporated in the rear axle to accommodate terrain-induced chassis deformation and improve ground contact.

Above the chassis, the external frame forms the primary structural interface for the rover's upper subsystems. Similar to the chassis, it is manufactured using SLM from AlSi10Mg and its geometry was derived with consideration of the expected mechanical loads. The remaining upper assemblies are mechanically integrated into this frame. The external frame itself is connected to the chassis through dedicated thermal-isolation elements, providing a mechanical interface while reducing conductive heat transfer between the locomotion system and the upper structure.

The inner frame accommodates the main electrical and electronic subsystems of the DM. These include the central control electronics, sensor units including the camera system, the battery pack, and a centralized electrical interface that integrates the subsystem power and signal connectors. For terrestrial operations, an active forced-air cooling system is additionally integrated into the inner frame to dissipate heat generated by the electronics.

The outer surface of the external frame is covered with a 3D-printed thin cover to protect the external frame and internal components, which serves as a placeholder for a future MLI thermal isolator.

The top frame includes spring-loaded quick-release antenna mechanisms, a radiator panel based on a multilayer carbon-fiber-reinforced polymer (CFRP) sandwich structure, and the solar-panel assembly. The terrestrial solar-panel configuration provides approximately 17 W of electrical power and uses a carbon-fiber-foam-reinforced sup-

Copyright © 2026 by Mehmed Yüksel. Published by the International Astronautical Federation (IAF), with permission and released to the IAF to publish in all forms. All rights reserved.

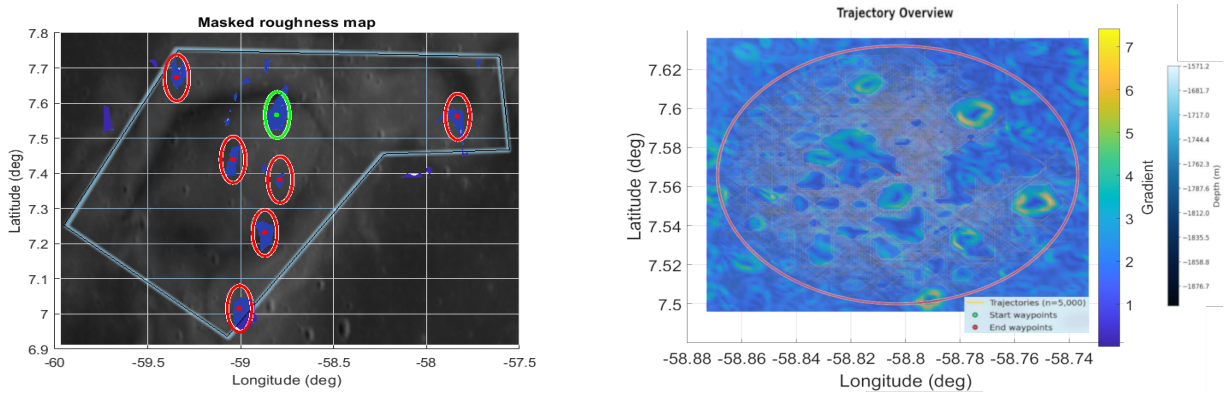


Fig. 2. LuNiS mission landing site selection phases: (left) region of interest determination on Reiner Gamma (Credits: Quickmap LRO) with roughness threshold mapping over the region of interest; (right) generated possible mission trajectories merged with gradient map of the selected landing ellipse.

porting structure with aluminum hinges. The top frame is connected to the external frame through thermal-isolation plates to reduce conductive heat transfer between the two structures.

3.3 LuNiS Thermal Model (TM)

The thermal design of the rover is supported by two complementary models. An analytical thermal model used to analyse the thermal behaviour of the flight configuration via simulation[9], and a physical thermal demonstrator used to experimentally validate the analytical thermal model and respective analyses. The demonstrator provides the experimental basis for correlating the analytical model with actual hardware behaviour under thermal vacuum conditions and solar-equivalent irradiation. This correlation enables the validation and refinement of key model assumptions, which can be transferred to the LuNiS V1 thermal model. This enables confident predictions of the actual flight performance.

The physical thermal demonstrator is manufactured at a 1:2 scale to comply with the available test facility and its operational constraints (see in Fig. 4). Scaling the thermal system requires particular considerations, as the relevant heat-transfer mechanisms do not scale uniformly with geometry. While conductive heat paths scale linearly with geometric dimensions, radiative heat transfer scales with surface area and thermal capacitance with volume. Consequently, the geometry and thermal interfaces are adapted selectively to preserve the dominant thermal behaviour of the full-scale rover rather than applying a purely geometric scaling approach. Since the steady-state temperature distribution is of particular interest, special care was taken to ensure that the conductances are scaled correctly.

The mechanical structure is realized using modular aluminum profiles to reduce manufacturing effort and facilitate rapid reconfiguration. In contrast, thermally critical components, including conductive isolations, wheel and motor assemblies, mechanisms and thermal interfaces, are reproduced as accurately as practicable to preserve representative conductive heat paths. To reproduce the relevant thermo-optical characteristics, space-grade materials and surface finishes for components such as the radiator, solar cells, and MLI are used. Instead of a thermal switch between the electronics box and the radiator, removable thermal straps are implemented. This facilitates the manual activation and deactivation of the heat path, imitating the variability of a thermal switch.

Overall, the thermal demonstrator is designed to reproduce the dominant thermal characteristics and heat paths of the flight configuration while remaining sufficiently modular for experimental adaptation. The resulting test platform enables systematic thermal testing for subsequent correlation of the analytical thermal model.

Copyright © 2026 by Mehmed Yüksel. Published by the International Astronautical Federation (IAF), with permission and released to the IAF to publish in all forms. All rights reserved.

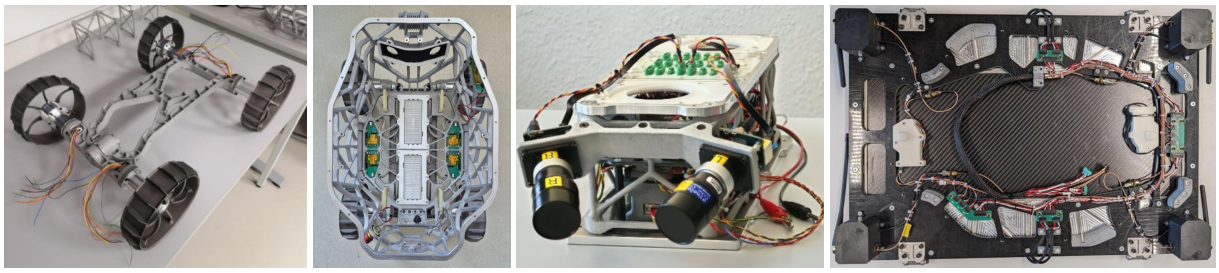


Fig. 3. Pictures from the electrical and mechanical assembly and integration steps of LuNiS DM within the SAMLER-KI project. *Left:* Chasis with titanium wheels and passive joint in the rear axle. *Middle-left:* The external frame (top view) as corpus. *Middle-right:* The inner frame with electronic assembly. *Right:* Top frame (bottom view), including antenna and solar panel deployment mechanisms.



Fig. 4. LuNiS TM for thermal-vacuum-testing.

4. Testing and Evaluation of Results

4.1 Tests with LuNiS DM

LuNiS-DM, as a functional demonstrator, is operated in the context of SamlerKI on terrestrial analogue environment. The goal is to gain first insights into the targeted system design, from both a hardware and software point of view. This serves as a verification step for the necessary system and control functions. It also provides insights for the next iteration of the space model V2.

LuNiS-DM was preliminarily tested in the snowy environment to observe whether LuNiS can continue his operation in a comparably cold environment (see in Fig. 5). The tests were carried out in the parkour area of DFKI-RIC Bremen. During the tests, the environmental temperature was −5 °C, which reduced the internal temperature of LuNiS-DM to −2.5 °C. The major outcomes of the tests are: (i) LuNiS-DM was proven to continue its operation at −2.5 °C, (ii) the wheels has enough handling for slippery terrain, (iii) a software bug related to clock synchronization due to low temperature was found and immediately resolved.



Fig. 5. LuNiS in snow tests carried out in DFKI-RIC outdoor test field.

To evaluate the mobility performance of the rover, four wheel configurations with different diameters and widths were tested under representative terrestrial conditions. The experiments included driving on flat terrain, tests with different payloads, slope-climbing tests, and rock and step obstacle traversal. Representative test scenarios are shown in Fig. 6, including traversal over a 12 cm rock obstacle and a 30° slope-climbing test.

After each experiment, the terrain surface was captured using a 3D laser scanner. The resulting point clouds, as illustrated in Fig. 6, were further processed in MATLAB to quantify the wheel-induced terrain deformation and determine parameters such as wheel sinkage and slip ratio. In parallel, motor voltage and current were recorded during the experiments to compare the electrical power consumption of the different wheel configurations.

The results show that the large-diameter, large-width wheel configuration provided the best overall mobility per-

Copyright © 2026 by Mehmed Yüksel. Published by the International Astronautical Federation (IAF), with permission and released to the IAF to publish in all forms. All rights reserved.

formance. In particular, this configuration exhibited the lowest sinkage and slip ratio, together with significantly lower electrical power consumption. This trend is consistent with classical terramechanics theory, according to which wheel sinkage depends on the applied wheel load, wheel geometry, and terrain properties [10]. For a given terrain and wheel load, increasing the wheel width and diameter can reduce sinkage and soil deformation by improving the wheel–soil contact conditions [11]. Under increased payload conditions, the large-diameter, large-width wheels maintained better mobility, whereas the smaller and narrower wheels exhibited greater sinkage and substantially higher slip. Wheel slip and the available tractive force are also influenced by the wheel–soil contact area, contact length, and soil shear properties [12].

For the purpose of the evaluation of the security, robustness, performance, and accuracy of the on-board software inside the rover, tests for the on-board software; Guidance, Navigation, and Control (GNC) module; telecommand and telemetry transactions with Ground Station were conducted both in laboratories, Crater, and Control Room in DFKI-RIC Bremen (see in Fig. 7). Crater Area facility provided lunar-analogue environment to test GNC module functionalities, teleoperation, and semi-autonomous operations.



Fig. 7. The facilities inside DFKI-RIC Bremen utilized for testing the on-board software on LuNiS: Crater Area on the left, Control Room on the right.

According to the test results and the evaluation reports, the major outcome is the fact that the rover is proven to be teleoperable and to enable the implementation of algorithms and decision units for autonomy. During the teleoperation tests, the rover threw errors related to both hardware and software at the runtime. However, the on-board software was enable to catch those errors and the users were able to recover without any special diagnosis process on the rover.

For the navigation aspects, the rover is able to estimate its position and attitude within acceptable entry levels. However, for the realistic scenarios, algorithms are needed to be optimized and improved for secure operations. Nevertheless, LuNiS is able to generate Digital Elevation Map (DEM) of the environment properly, when the navigation output is well-aligned at the specific lighting conditions. In the context of AI-Based obstacle detection, the FPGA module provided enough resources for the kernel placement and it accomplished the tasks of obstacle detection. However, since the lighting condition affects the accuracy of the algorithm, the adjustment of the model to different lighting conditions was found to be necessary.

4.2 Tests with LuNiS TM

The LuNiS TM thermal demonstrator (see in Fig. 4) was used for thermal testing. A vacuum chamber equipped with a liquid nitrogen thermal shroud provided the radiative environment. To simulate the lunar surface temperature regime below and around the rover, the ground plate was temperature controlled via heated gaseous nitrogen.

Additional to the night case without any external illumination, several illumination cases were tested as well in order to investigate the thermal behaviour under solar illumination. For this purpose, the rover was illuminated by a large scale solar simulator in predefined attitudes.

For each test case, a defined heating power was applied to the electronics mass dummy within the inner box of the rover, considering power losses in the harness. Several PT100 temperature sensors in four wire measurement configuration measured the temperatures in front of and behind critical heat paths. This way, the thermal conductivities of these heat paths could be calculated afterwards during correlation. Steady state temperatures were always recorded after temperatures settled sufficiently.

The measured temperature values of all test cases were utilized to correlate the thermal model of the LuNiS TM thermal demonstrator to an accuracy of $< \pm 10\,K$ at relevant locations. The findings obtained and adjustments made during the correlation process were then transferred to the thermal model of the LuNiS V1 space system. This enables predictions of the actual thermal behaviour under relevant environmental flight conditions.

Copyright © 2026 by Mehmed Yüksel. Published by the International Astronautical Federation (IAF), with permission and released to the IAF to publish in all forms. All rights reserved.



Fig. 6. Terrestrial mobility and terrain-interaction tests of the LuNiS DM. Left: Traversal over a 12 cm rock obstacle. Middle-left: Mobility test on a 30° slope. Middle-right: Point cloud of the test terrain acquired using 3D laser scanning. Right: MATLAB-based analysis of the terrain sinkage.

5. Lesson Learned and iteration LuNiS V2

The lessons learned from the structural and thermal analyses, together with the semi-autonomous function tests conducted at the DFKI-RIC crater test field and in outdoor analog-environment trials, have informed the identification of open points, at the mission, requirement, and system design levels, that must be addressed in the next iteration.

5.1 Lessons Learned from LuNiS DM

The major change in LuNiS-DM with respect to the previous design is the change of design philosophy, which also enable multi night survival on the moon surface. The previous design iteration was merely based on the cost-optimization with a night survival capability of single lunar night. In comparison to the previous iteration, we applied ECSS margin philosophy [13] to the design, in order to allocate space for any design and implementation errors without affecting the whole design process. The changes in the other aspects of the design followed this philosophy change accordingly.

The major drawback of the cost-optimized design was the elimination of redundancies wherever possible, which increased the risk factor for the mission operations. Within the change in design philosophy, redundancies in components and modules were added in the design. In addition, since the power input requirement for maintaining the LuNiS internal temperature at operational levels is also reiterated, more batteries were needed to provide the enough power throughout the lunar night. Another factor is the mass, volume, power, and temporal allocations for payload unit are also increased in LuNisV2. As a result, the overall mass of the rover increased from 20.7 to 59.4 kg. The sectionwise mass increase is given in Table 1.

Section / Mass	Lunis v1 (kg)	Lunis v2 (kg)
Chassis	2.8	7.9
Structure	5.5	15.7
Electronics	8.1	26.5
Top Frame	3.6	7.4
Harness	0.7	1.9
Total	**20.7**	**59.4**

Table 1. Mass budget table distributed to the sections of LuNiS along the comparison with the previous version

In the previous design, it was found out that the major driver on the rover mass is the batteries, due to the requirement of single lunar night survivability [4]. In this sense, the combination of primary and secondary cells were considered for the design, in which primary cells undertake the night-time survivability, and secondary cells were found to be more suitable for day-time operations. This decision saved 4.14 kg of mass, which became substantial considering the rover with 20.7 kg overall mass. The mass increase in LuNiS v2 caused the attraction for the requirement for lunar night survivability to switch from single night to multi night. After the trade-off study, it was decided to build the rover with multi lunar night survival capability, since it adds only 9.99 kg to the mass budget.

The wheel design and validation process also provided an important lesson for the locomotion system. Four configurations with different wheel diameters and widths were

Copyright © 2026 by Mehmed Yüksel. Published by the International Astronautical Federation (IAF), with permission and released to the IAF to publish in all forms. All rights reserved.

tested under representative conditions, including different payloads, deformable terrain, slope climbing, and rock and step obstacle traversal. In addition to the mobility performance, the resultant sinkage and slip ratio were evaluated from the measured wheel motion and 3D terrain scans, while the electrical power consumption of the drive units was recorded. The experiments showed that the large-diameter, large-width wheel configuration provided the best overall performance, with lower sinkage and slip as well as lower electrical power consumption. The difference became particularly evident under increased payload, where the smaller and narrower wheels experienced significantly larger sinkage and slip. A key lesson from those tests is that wheel selection should not be driven by mass and compactness alone. Wheel diameter and contact area strongly influence terrain interaction, traction, and drive power. The tests also highlighted the importance of validation under representative terrain and payload conditions, where differences between wheel configurations became significantly more pronounced.

Lifting the hard mass-optimization requirement enabled more functionalities in navigation aspects. In the previous design, the minimal configuration for the navigation possible, which fuses visual odometry from stereo cameras, imu, and wheel odometry, was suggested [4]. The most well-known drawback of this configuration is the drift accumulated both in IMU and Visual Odometry output, which makes the deviation in both position and attitude estimations from the actual values. Therefore, sun sensors are integrated in the design to eliminate the drift in attitude and position estimation. In addition, during the tests, it was also found out that, the rover can find itself in situations, when the backwards motion is the only solution. In those situations the cameras only at the front side might become significantly risky for the operation. Therefore, two stereo cameras are added at the backside of the rover for navigation, and two engineering cameras were distributed into both sides of LuNiS.

During the tests for mission operations, the rover was placed inside the crater area, while being controlled and steered by engineers in the mission control room in DFKI-RIC. These tests provided insights about the possible failure cases coming from all submodules during the mission, such as communication module failures/blackouts, motor failures, blackouts in field of view, data transfer corruption, state machine failures in on-board software, hardships in steering with delayed communication, and more importantly the true sense that the rover is not reachable anymore after the launch for the diagnosis and maintenance. Therefore, failures that are detected during the tests but left unprecedented or open were included in Fault Detection Isolation and Recovery (FDIR) registry in on-board software, and then the mitigation methodology was implemented correspondingly.

The on-board software inside LuNiS-DM was migrated from research oriented application towards safety-critical application, due to the bugs and failures detected during tests for mission operations and the navigation. Especially software blocks that has been proposed in the previous iteration [4] that forced the on-board software to use dynamic memory allocation, was acceptable for research purposes, while being prohibited in space missions [14], since it obscures error tracking, unprecedented error propagation, and requires special units for heap memory overflow [15]. In addition, those modules did not function robust and reliable during our tests, which accelerated the migration from the research-oriented modules to the self-implemented and compact modules, which were proven to be robust and reliable in following tests.

5.2 Lessons Learned from LuNiS TM

Regarding the thermal design, a number of aspects came up that are considered noteworthy. The radiative heat loss via the top panel surrounding the radiator turned out to be larger than assumed. Even though the radiator was conductively decoupled from the surrounding top panel, a significant amount of heat leakage occurred in cold case conditions. Closing the solar panels during the cold night produces significant benefits with a reduction in power loss by 17 %. A second successful approach to mitigate heat loss via the top panel is the use of sandwich panels with low conducting honeycomb material, e.g. Nomex or Kevlar. Additionally to MLI, this presents a further isolation of the top panel surface from the underlying structure.

The testing campaign highlighted several limitations associated with the use of a scaled thermal demonstrator. Although scaling provides advantages regarding manufacturing cost and test facility constraints, the measured results cannot be directly transferred to the full-scale configuration. This holds in particular for the transient thermal behaviour which is highly affected by changes in ther-

Copyright © 2026 by Mehmed Yüksel. Published by the International Astronautical Federation (IAF), with permission and released to the IAF to publish in all forms. All rights reserved.

mal mass, conductive paths, and surface-to-volume ratios. Also the conductive heat paths of individual components can exhibit unscalable thermal effects, besides the inherent difficulty of assessing their thermal through-conductance. Bearings, for example, may show different thermal behaviour as their geometry and contact conditions change significantly with scale.

Another major challenge was reproducing representative solar illumination conditions. The available test facility was equipped with a solar simulator, but the actual illumination level at the demonstrator was not known with sufficient accuracy. Uncertainties in this boundary condition directly affect the comparability between test results and numerical predictions.

Finally, the available testing time limited the ability to reach steady-state conditions. The achieved temperature states could not be classified as steady state according to the applicable European Cooperation for Space Standardization (ECSS) criteria. Although a larger number of test cases provides broader experimental coverage, longer test durations with fewer, carefully selected cases are considered preferable.

5.3 Adaptations LuNiS V2 (space variant)

Based on the test results and the newly established budgets, a new iteration of the LuNiS rover was designed. The main drivers for this change were a new requirement for multi-night survival and the integration of the payload into the interior of the rover so that it, too, could survive the lunar night.

To achieve multi-night survival, the battery design was revised to include a single large secondary battery that provides enough energy to heat the rover overnight and can be recharged during the day. The design featuring a two-layer MLI and a structure consisting of an outer body and an inner body was retained. To optimize thermal management, the electronics in the inner body were completely isolated from the battery, and only the electronics were connected to the radiator on the top panel via thermal switches. This is intended to minimize heat loss from the battery overnight, as the battery is the most critical component for nighttime survival. In addition, a preliminary selection of possible components for the electronics has already been made, and a specific layout within the electronics box has been planned. Factors such as compatibility with radiation were taken into account in this process.

A dedicated compartment was designed inside the rover for the payload, which is connected to the inner body in an isolated manner. This compartment makes it possible to install or replace a 2U-sized payload in the rover even after the entire rover has been assembled. The payload is located on the front lower side of the rover and could potentially be equipped in the future with a window facing forward or downward for scientific measurements.

The thermal analysis of the previous design showed that the top panel represented a significant heat path to the external environment. Consequently, reducing heat transfer through the top panel became an important design consideration for the new iteration. In addition to the thermal isolation of the battery, the possibility of reducing conductive heat losses through the use of thermally isolating sandwich structures is considered. Additionally, in the new version, actuated solar panels are installed on the top panel, which can be actively oriented toward the sun and closed overnight to minimize heat radiation through the radiator. Moreover, sun sensors will be installed on the top panel to optimize the rover's navigation and orientation. Additional cameras are planned for the rear of the rover to aid in navigation, as well as two hazard cameras, each facing to the side of the rover to detect obstacles in front of the wheels. The wheels themselves were modified based on the test results, and their diameter was significantly increased.

The chassis in combination with the thermal brackets was found out to be one of the most critical components. Thus, the design was revised, resulting in the use of single wheel suspension at the front and the swing axle at the rear being mounted directly to the outer body via an isolated interface. This made it possible to significantly reduce the size and, consequently, the relative weight of the chassis. In addition, the launch locks were mounted directly on the outer body, allowing the launch forces to act closer to the rover's center of gravity and significantly reducing the loads on the chassis and any connecting brackets. By transferring the launch loads more directly into the outer body, thermal insulation brackets only need to hold the weight of the inner components and therefore can be relieved.

Taken together, these modifications resulted in a significant increase in the rover's size and weight, which is primarily due to the decision to enable multi-night survival and the integration of the payload. As a result, LuNiS V2

Copyright © 2026 by Mehmed Yüksel. Published by the International Astronautical Federation (IAF), with permission and released to the IAF to publish in all forms. All rights reserved.

measures approximately 895 mm x 610 mm x 500 mm with the panels closed and weighs less than 50 kg. When the panels are extended, the height can reach up to 685 mm and the width up to 810 mm.

6. Conclusion and Future Work

Due to additional objectives identified for the upcoming design cycle, specifically a revised thermal subsystem design accompanied by a new thermal demonstration campaign, together with parallel goals in the software and AI domains, most notably in Fault Detection, Isolation, and Recovery (FDIR), the SAMLER-KI project has been granted a budget increase and a one-year extension.

As presented in this paper, the design process of the LuNiS rover has been completed. Its integration has likewise been finalized, and the system has been put into service as a functional demonstrator for ground-based functional testing, where it is now being used for software and AI verification activities.

The Samler-KI project is scheduled for completion in October 2027. The next phase is planned to complete two further design cycles incorporating the updated space model, thereby advancing the subsystem-level technology readiness level (TRL) of the SAMLER-KI planetary rover concept, in particular for the locomotion and navigation subsystems, while other subsystems are still kept to be defined.

Acknowledgements

This work has been carried out within the project SAMLER-KI (grant no. 50RA2203A), which is funded by DLR with federal funds of the Federal Ministry of Research, Technology and Space in accordance with the parliamentary resolution of the German Parliament. The authors are grateful for the support of the SAMLER-KI project team as well as all the supporting staff at the DFKI-RIC and the FH Aachen Space technology department

[1] J. Walker, L.-J. Burtz, F. Dubois, A. Calzada-Diaz, and T. Tanaka, "Ispace modular rover design," in *IAC-19, 70th International Astronautical Congress, Washington, DC, USA*, Oct. 2019.

[2] T. Oikawa et al., "Plan and progression of the technology readiness level of the cuberover," in *IAC-23, 74th International Astronautical Congress, Baku, Azerbaijan*, Oct. 2023.

[3] E. R. Jawin, S. N. Valencia, R. N. Watkins, J. M. Crowell, C. R. Neal, and G. Schmidt, "Lunar science for landed missions workshop findings report," *Earth and Space Science*, vol. 6, no. 1, pp. 2–40, 2019. DOI: https://doi.org/10.1029/2018EA000490. eprint: https://agupubs.onlinelibrary.wiley.com/doi/pdf/10.1029/2018EA000490. [Online]. Available: https://agupubs.onlinelibrary.wiley.com/doi/abs/10.1029/2018EA000490.

[4] M. Yüksel et al., "Development of a semi-autonomous microrover for lunar night survival," Jan. 2024, pp. 214–228. DOI: 10.52202/078357-0028.

[5] M. Kurata, H. Tsunakawa, Y. Saito, H. Shibuya, M. Matsushima, and H. Shimizu, "Mini-magnetosphere over the reiner gamma magnetic anomaly region on the moon," *Geophysical Research Letters*, vol. 32, no. 24, 2005. DOI: https://doi.org/10.1029/2005GL024097. eprint: https://agupubs.onlinelibrary.wiley.com/doi/pdf/10.1029/2005GL024097. [Online]. Available: https://agupubs.onlinelibrary.wiley.com/doi/abs/10.1029/2005GL024097.

[6] E. S. Service, *Moon tiled dsk file for 59m sldem usgs v1 surface*, Dataset, version 1.0, ESA Cosmos, 2025. Accessed: Aug. 25, 2026.

[7] C. H. Acton, "Ancillary data services of nasa's navigation and ancillary information facility," *Planetary and Space Science*, vol. 44, no. 1, pp. 65–70, 1996, Planetary data system, ISSN: 0032-0633. DOI: https://doi.org/10.1016/0032-0633(95)00107-7. [Online]. Available: https://www.sciencedirect.com/science/article/pii/0032063395001077.

[8] C. Acton, N. Bachman, B. Semenov, and E. Wright, "A look towards the future in the handling of space science mission geometry," *Planetary and Space Science*, vol. 150, pp. 9–12, 2018, Enabling Open and Interoperable Access to Planetary Science and Heliophysics Databases and Tools, ISSN: 0032-0633. DOI: https://doi.org/10.1016/j.pss.2017.02.013. [Online]. Available:

Copyright © 2026 by Mehmed Yüksel. Published by the International Astronautical Federation (IAF), with permission and released to the IAF to publish in all forms. All rights reserved.

https://www.sciencedirect.com/science/article/pii/S0032063316303129.

[9] L. Spies, J. Gützlaff, D. Zinken, and M. Czupalla, "A thermal and structural assessment of a conceptual lunar micro rover design with the aim of night survivability," *Engineering Proceedings*, vol. 90, no. 1, 2025, ISSN: 2673-4591. DOI: 10.3390/engproc2025090093. [Online]. Available: https://www.mdpi.com/2673-4591/90/1/93.

[10] D. Akin, *Planetary surface robotics: Terramechanics 1*, https://spacecraft.ssl.umd.edu/academics/788XF20/788XF20L06.terramechanics1x.pdf, 2020.

[11] J. Y. Wong, *Theory of Ground Vehicles*, 4th. John Wiley & Sons, 2008.

[12] D. Akin, *Planetary surface robotics: Terramechanics 2*, https://spacecraft.ssl.umd.edu/academics/788XF20/788XF20L07.terramechanics2x.pdf, 2020.

[13] ESA, "Margin philosophy for science assessment studies," 2012.

[14] G. Holzmann, "The power of 10: Rules for developing safety-critical code," *Computer*, vol. 39, no. 6, pp. 95–99, 2006. DOI: 10.1109/MC.2006.212.

[15] Jet Propulsion Laboratory, "Jpl institutional coding standard for the c programming language," Jet Propulsion Laboratory, California Institute of Technology, Tech. Rep. JPL DOCID D-60411, 2009, Version 1.0.